Inorganic Chemistry

Article

pubs.acs.org/IC

Density Functional Theory Mechanistic Study of the Reduction of CO_2 to CH_4 Catalyzed by an Ammonium Hydridoborate Ion Pair: CO_2 Activation via Formation of a Formic Acid Entity

Mingwei Wen, Fang Huang, Gang Lu, and Zhi-Xiang Wang*

School of Chemistry and Chemical Engineering, University of the Chinese Academy of Sciences, Beijing 100049, China

Supporting Information

ABSTRACT: Density functional theory computations have been applied to gain insight into the CO_2 reduction to CH_4 with Et_3SiH, catalyzed by ammonium hydridoborate **1** ($[TMPH]^+[HB(C_6F_5)_3]^-$, where TMP = 2,2,6,6-tetramethylpiperidine) and $B(C_6F_5)_3$. The study shows that CO_2 is activated through the concerted transfer of $H^{\delta+}$ and $H^{\delta-}$ of **1** to CO_2, giving a complex (**IM2**) with a well-formed HCOOH entity, followed by breaking of the O−H bond of the HCOOH entity to return $H^{\delta+}$ to TMP, resulting in an intermediate **2** ($[TMPH]^+[HC(=O)OB(C_6F_5)_3)]^-$), with CO_2 being inserted into the B−H bond of **1**. However, unlike CO_2 insertion into transition-metal hydrides, the direct insertion of CO_2 into the B−H bond of **1** is inoperative. The computed CO_2 activation mechanism agrees with the experimental synthesis of **2** via reacting HCOOH with TMP/$B(C_6F_5)_3$. Subsequent to the CO_2 activation and $B(C_6F_5)_3$-mediated hydrosilylation of **2** to regenerate the catalyst (**1**), giving $HC(=O)OSiEt_3$ (**5**), three hydride-transfer steps take place, sequentially transferring $H^{\delta-}$ of Et_3SiH to **5** to $(Et_3SiO)_2CH_2$ (**6**, the product of the first hydride-transfer step) to Et_3SiOCH_3 (**7**, the product of the second hydride-transfer step) and finally resulting in CH_4. These hydride transfers are mediated by $B(C_6F_5)_3$ via two S_N2 processes without involving **1**. $B(C_6F_5)_3$ acts as a hydride carrier that, with the assistance of a nucleophilic attack of **5**−**7**, first grabs $H^{\delta-}$ from Et_3SiH (the first S_N2 process), giving $HB(C_6F_5)_3^-$, and then leave $H^{\delta-}$ of $HB(C_6F_5)_3^-$ to the electrophilic C center of **5**−**7** (the second S_N2 process). The S_N2 processes utilize the electrophilic and nucleophilic characteristics possessed by the hydride acceptors (**5**−**7**). The hydride-transfer mechanism is different from that in the CO_2 reduction to methanol catalyzed by N-heterocyclic carbene (NHC) and PCP-pincer nickel hydride ([Ni]H), where the characteristic of possessing a C=O double bond of the hydride acceptors is utilized for hydride transfer. The mechanistic differences elucidate why the present system can completely reduce CO_2 to CH_4, whereas NHC and [Ni]H catalysts can only mediate the reduction of CO_2 to [Si]OCH_3 and $catBOCH_3$, respectively. Understanding this could help in the development of catalysts for selective CO_2 reduction to CH_4 or methanol.

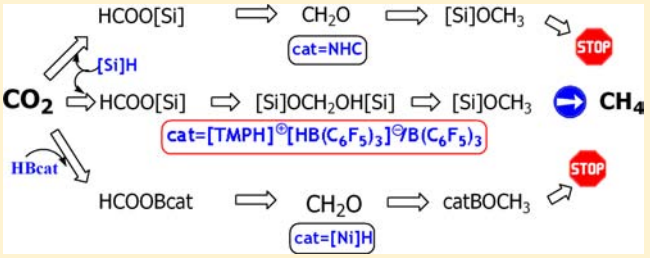

1. INTRODUCTION

The rising concentration of atmospheric carbon dioxide (CO_2) is one of the major factors responsible for global climate change. Yet, CO_2 can serve as an abundant, inexpensive, and renewable C1 source to synthesize useful chemicals, attracting considerable effort to develop catalytic routes for CO_2 conversion.[1−3] These studies, on the one hand, may help in finding solutions to large-scale CO_2 applications. On the other hand, because CO_2 conversion is challenging as a result of its great stability, the knowledge learned from how to tame so stable a molecule could spark ideas to discover novel catalytic approaches for other molecular transformations. Among many possible CO_2 transformations, the reduction to fuel molecules such as methanol[4−10] and methane (CH_4)[11−15] has been proposed to be a promising way to utilize the refractory molecule. Interestingly, both homogeneous transition-metal (TM)-based and metal-free catalytic systems have been found to be capable for such transformations. Regarding conversion to CH_4, five catalytic systems have been developed. In 2006, Matsuo and Kawaguchi used the zirconium(IV) dibenzyl complex and $B(C_6F_5)_3$ to reduce CO_2 to CH_4 with various silanes as the reductant.[11] Brookhart et al. developed an efficient PCP pincer iridium-complex catalyst to reduce CO_2 to CH_4 with trialkysilanes as the reductant.[12] Mitton and Turculet reported that the palladium or platinum silyl pincer complexes in combination with $B(C_6F_5)_3$ can efficiently catalyze the CO_2 conversion to CH_4 with a tertiary silane as the reducing agent.[13] Piers et al. demonstrated the metal-free ammonium hydridoborate ion pair **1** {$[TMPH]^+[HB(C_6F_5)_3]^-$ (the hydrogen activation product by a TMP/$B(C_6F_5)_3$ frustrated Lewis pair (FLP), where TMP = 2,2,6,6-tetramethylpiperidine[16])} in combination with $B(C_6F_5)_3$ could catalytically transform CO_2 to CH_4 with silane as the hydrogen source.[14] Khandelwal and Wehmschulte reported that strong Lewis acids such as $[Et_2Al]^+$

Received: July 24, 2013
Published: October 2, 2013

and $[R_3Si]^+$ can catalyze the reduction of CO_2 to CH_4 with silanes (e.g., Et_3SiH).[15]

Previously, we have studied the mechanisms of CO_2 conversion into CH_3OH mediated by N-heterocyclic carbene (NHC)[9] and PCP-pincer nickel hydride ([Ni]H)[10] catalysts, respectively. In connection with our interest in FLP[17] and CO_2 conversion chemistry,[9,10] we herein present an in-depth mechanistic study on the **1**-catalyzed CO_2 reduction to CH_4 by trialkysilane, developed by Piers et al.[14] Specifically, we are interested in the CO_2 activation mode and why the current system completely reduces CO_2 to CH_4, whereas the [Ni]H[6] and NHC[7] catalysts can only partially reduce CO_2 to give $catBOCH_3$ and $[Si]OCH_3$, respectively.

2. COMPUTATIONAL DETAILS

Using experimental compounds rather than simplified models, all structures were optimized in the gas phase at the M05-2X[18]/6-31G* level. The choice of the M05-2X functional is based on its successful application in describing the mechanism of CO_2 reduction to methanol with silane, catalyzed by NHC.[9] Harmonic-frequency-analysis calculations were then performed to verify the optimized structures as minima (no imaginary frequency) or transition states (TSs, having one unique imaginary frequency). The energies were then improved by M05-2X/6-311++G**//M05-2X/6-31G* single-point calculations with solvent effects accounted for by the SMD[19] solvent model, using the experimental solvent (bromobenzene). The refined energies were then corrected to obtain enthalpies and free energies at 298.15 K and 1 atm, using the gas-phase M05-2X/6-31G* harmonic frequencies. It should be emphasized that such thermal corrections based on the ideal gas-phase model inevitably overestimate entropy contributions to free energies for reactions in solvent, in particular for reactions involving component changes, because the suppressing effect of the solvent on the rotational and transitional freedoms of the substrates is ignored. Because no standard quantum-mechanics-based approach is available for accurate prediction of the entropy in solution, we adopted the approximate approach proposed by Martin et al.[20] According to their approach, a correction of 4.3 kcal/mol applies per component change for a reaction at 298.15 K and 1 atm [i.e., a reaction from m to n components has an additional correction of $(n - m) \times 4.3$ kcal/mol]. In agreement with this approach, Rybak-Akimova et al.[21] found a 4−5 kcal/mol overestimation of the entropic contribution by comparing the experimental and computed values for the CO_2 fixation by nickel(II) hydroxide complexes. In the following discussion, we use the free energies corrected by Martin et al.'s approach and give the enthalpies for references in the brackets in the relevant figures. Because the system is large (up to 125 atoms), and it is time-consuming and difficult to optimize TSs in the flat region of the potential energy surface, we omitted some trivial TSs and indicate the probably missed TSs with dashed lines in the free-energy profiles. Natural bond orbital (NBO)[22] analyses were performed at the M05-2X/6-31G* level to assign atomic charges (Q). All calculations were performed using the *Gaussian 09* program.[23] All optimized structures, as well as their Cartesian coordinates, are given in the Supporting Information.

3. RESULTS AND DISCUSSION

3.1. Reduction Mechanism of CO_2 to CH_4. On the basis of the observed intermediates, Piers et al. have postulated a mechanism for their CO_2 reduction to CH_4 (Scheme 1).[14] The whole reduction can be characterized by three stages, including (stage I) CO_2 activation by **1** to give the ammonium formatoborate ($[TMPH]^+[HC(=O)OB(C_6F_5)_3]^-$, **2**), (stage II) hydrosilyation of **2** mediated by $B(C_6F_5)_3$, regenerating the catalyst **1** and giving the formatosilane ($HC(=O)OSiEt_3$, **5**), and (stage III) three sequential $B(C_6F_5)$-mediated hydrosilyations, leading **5** to $(Et_3SiO)_2CH_2$ (**6**), then to Et_3SiOCH_3 (**7**), and finally to CH_4. We describe our computational results in terms of the three stages. In a single catalytic cycle, the reduction of CO_2 to CH_4 involves one **1** and one $B(C_6F_5)_3$ as the catalysts, respectively, and four Et_3SiH molecules. The free energies discussed below are all relative to the total free energy of **1** + $B(C_6F_5)_3$ + CO_2 + $4Et_3SiH$, unless otherwise specified.

Scheme 1. Schematic Mechanism of CO_2 Reduction to CH_4 Postulated by Piers et al.[14]

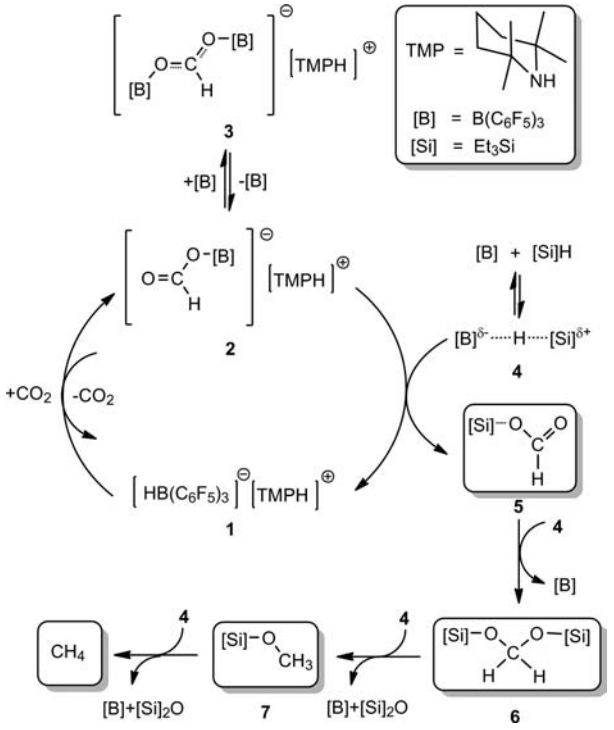

*Stage I: CO_2 Activation by the Ion Pair **1**.* CO_2 is an exceptionally stable molecule; thus, its activation is often the critical step for its conversion. Experimentally, it has been demonstrated that introducing CO_2 to the solution of **1** gives **2**, with CO_2 being inserted into the B−H bond of the $[HB(C_6F_6)_3]^-$ component of **1**.[8,14] Figure 1 illustrates our computed mechanism of how the CO_2 activation/insertion takes place, together with the energetic and geometric results. The CO_2 activation proceeds by its initial binding to **1** to form a complex **IM1** in which the $C^{\delta+}$ and $O^{\delta-}$ of CO_2 respectively interact with $H^{\delta-}$ and $H^{\delta+}$ of **1** via electrostatic interaction. The binding is favorable by 2.7 kcal/mol in enthalpy but unfavorable by 2.5 kcal/mol in free energy because of the entropy penalty. Subsequently, the $N-H^{\delta+}$ and $B-H^{\delta-}$ bonds of **1** break via **TS1** with a relative energy of 26.8 kcal/mol, and concomitantly $H^{\delta+}$ and $H^{\delta-}$ of **1** transfer to CO_2 to give **IM2** with a well-formed HCOOH entity. Previously, Musgrave et al. proposed HCOOH to be an intermediate for the CO_2 reduction with ammonia−borane as reducing agent.[3k] However, the HCOOH entity cannot be liberated because the products (free HCOOH + TMP/$B(C_6F_5)_3$) are 21.8 kcal/mol less stable than **1** + CO_2. Instead, **IM2** crosses a very low barrier (**TS2**) of 1.1 kcal/mol to transform to the much more stable ammonium formatoborate **2′**, which is 15.9 kcal/mol more stable than **1** + CO_2. The driving force for the transformation from **IM2** to **2′** is the donor−acceptor interaction between the B and O atoms of $B(C_6F_5)_3$ of the HCOOH moiety. Interestingly, as the B−O dative bond forms, the newly formed O−H bond of the

dx.doi.org/10.1021/ic401920b | *Inorg. Chem.* 2013, 52, 12098−12107

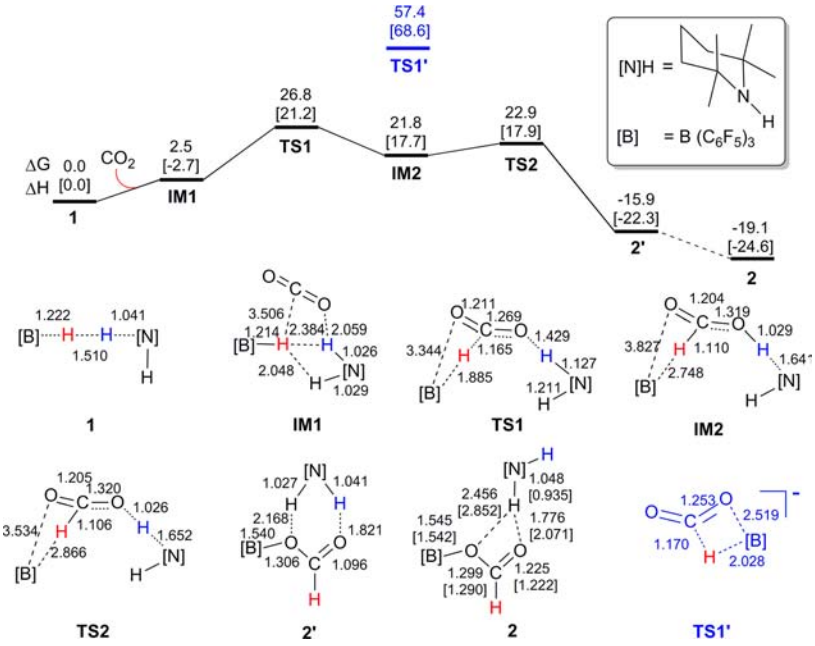

Figure 1. Free-energy (in kcal/mol) profile for CO_2 activation by **1**, along with the optimized structures of stationary points. Key bond lengths are given in angstroms. The values in parentheses in **2** are from its X-ray structure.

HCOOH moiety in **IM2** breaks and $H^{\delta+}$ returns to TMP; the O−H and N−H bond lengths (1.029 and 1.641 Å, respectively) in **IM2** are now changed to 1.821 and 1.041 Å in **2′**, respectively. The CO_2 activation product **2′** was optimized in the gas phase, with a starting structure generated by the slight displacement of **TS2** along the harmonic vibrational motion in the forward reaction direction. **2′** is related to the experimentally observed **2** but geometrically different from the X-ray structure of **2**.[8] We also optimized a structure using the X-ray structure of **2** as an initial geometry. In the gas phase, **2′** is 2.1 kcal/mol more stable than **2** but 3.2 kcal/mol less stable in solvent. Therefore, **2** is preferred in the solvent. We did not attempt to locate the TS between **2** and **2′** and assume that **2′** can easily transform of **2** by the swing of $[TMPH]^+$ because the transformation only needs to slightly alter the weak nonbonding interactions. Relative to **1** + CO_2, the CO_2 activation to give **2** overcomes a barrier of 26.8 kcal/mol and is exergonic by 19.1 kcal/mol. The barrier height for the forward reaction from **1** + CO_2 to **2** is in accordance with the experimental reaction conditions (2−4 atm and 56.0 °C in Piers et al.'s experiment[14] or 1 atm and 100.0 °C in Ashley et al.'s experiment[8]). Experimentally, it has been observed that 2% of **2** could be dissociated to release CO_2 under the conditions of 80.0 °C and 1 atm.[8] The barrier for the reverse reaction, 45.9 kcal/mol (the free-energy difference between **TS1** and **2**), is in reasonable agreement with the experimental observation. The somewhat high reverse barrier could be due to overestimation of the nonbonding interaction by the M05 functional, as reflected by the more compact computed structure (**2**) than the experimental X-ray structure, as compared in Figure 1. Nevertheless, the CO_2 activation mechanism is supported by the experimental facts that **2** could be synthesized independently via the reaction of formic acid with TMP/$B(C_6F_5)_3$,[8] and similarly Mayer et al. could synthesize the lutidinium formatoborate salt $[LutH]^+[HC(=O)OB(C_6F_5)_3]^-$ from formic acid and lutidine/$B(C_6F_5)_3$ FLP.[24]

The CO_2 insertion into the B−H bond of **1** is realized via two separate steps, including concerted $H^{\delta+}$ and $H^{\delta-}$ transfer via **TS1** and B−O dative bond formation via **TS2**. The B−O bond in **IM2** is far from being formed with a long B−O distance (3.827 Å), indicating that CO_2 does not insert into the B−H bond of **1** in the process from **1** to **IM2**. It has been known that the CO_2 activation by TM hydrides such as [Ni]H[6] often takes place via the direct insertion of CO_2 into the TM−H bond, resulting in a TM−OC(=O)H linkage in which the TM−O and C−H bonds form simultaneously.[2c,5,6,25] We also explored the direct insertion pathway; however, geometric optimizations to locate corresponding TSs always converged to **TS1**. Nevertheless, **TS1′** for CO_2 insertion into the B−H bond of the isolated $[HB(C_6F_5)_3]^-$ could be obtained (see Figure 1); the barrier for the insertion via **TS1′** is 57.4 kcal/mol relative to CO_2 + $[HB(C_6F_5)_3]^-$, which is 30.6 and 34.5 kcal/mol higher than **TS1** and **TS2**, respectively. We speculated that CO_2 cannot directly insert into the B−H bond of $[HB(C_6F_5)_3]^-$ of **1**. The ammonium $[TMPH]^+$ offers a detour for CO_2 insertion into the H−B bond of $HB(C_6F_5)_3$. The catalytic effect of $[TMPH]^+$ acts through its $H^{\delta+}$ interaction with CO_2, which enhances the electrophilicity of C^{CO_2} (we herein and hereafter use C^{CO_2} and O^{CO_2} to represent the C and O atoms stemming from CO_2) to accept $H^{\delta-}$ from $[HB(C_6F_5)_3]^-$ of **1**. Consistently, the C atom starts to bear more positive charge in **IM1** (1.102e) than in free CO_2 (1.067e).

*Stage II: Hydrosilyation of **2** To Regenerate the Catalyst **1** and Give Formatosilane **5**.* The CO_2 activation by **1** results in **2**. Experimentally, it has been found that the catalytic system requires additional borane $B(C_6F_5)_3$ to proceed. Previously, various $B(C_6F_5)_3$-catalyzed hydrosilylations have been developed.[26,27] Figure 2 illustrates the pathway for the hydrosilylation of **2** mediated by $B(C_6F_5)_3$. $B(C_6F_5)_3$ activates Et_3SiH by forming a complex **4** $[Et_3Si\cdots H\cdots B(C_6F_5)_3]$[25] in which the Si···H and H···B distances are 1.567 and 1.445 Å, respectively. The activation is exergonic by 6.7 kcal/mol relative to $B(C_6H_5)_3$ + Et_3SiH and makes the Si center of Et_3SiH more

dx.doi.org/10.1021/ic401920b | Inorg. Chem. 2013, 52, 12098−12107

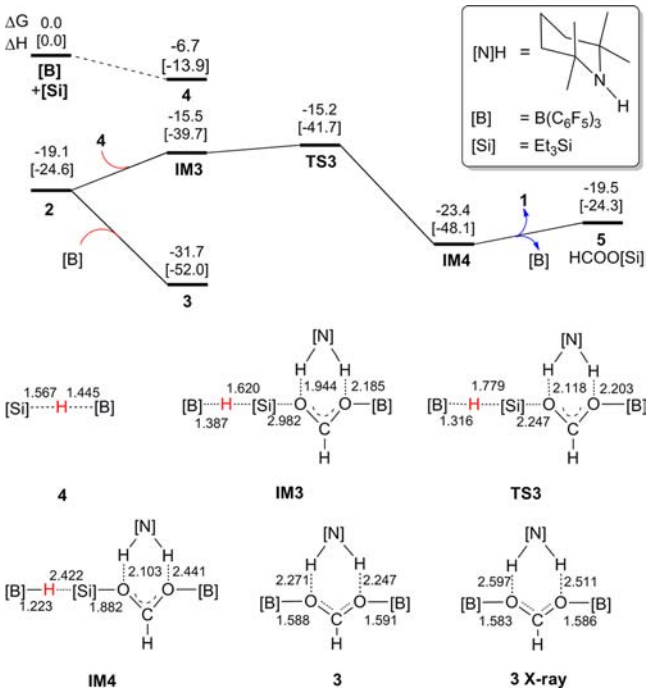

Figure 2. Free-energy (in kcal/mol) profile for the hydrosilylation of **2** to regenerate the catalyst, along with the optimized structures of stationary points. Key bond lengths are given in angstroms.

electrophilic and exposed for nucleophilic attack by **2**, as revealed by the larger positive charge of the Si center in **4** (1.895e) than in Et_3SiH (1.527e). For nucleophilic attack of **2** to **4**, we first considered two attacking models, including the following: (a) the exposed O atom of **2** attacks **4** at the Si center with Si−O bond formation and hydride transfer from **4** to C^{CO_2} taking place concertedly; (b) the exposed O atom of **2** attacks **4** to form the Si−O bond first, and then the resulting $[HB(C_6F_5)_3]^-$ gives $H^{\delta-}$ to C^{CO_2} with the least motion. However, both models were found inoperative because the two $B(C_6F_5)_3$ moieties in **4** $[Et_3Si\cdots H\cdots B(C_6F_5)_3]$ and **2** are too crowded. We here mention that a TS for model b could be located in the scenario of less crowding but is less favorable than the alternative (see below for more details about the attacking model). The mechanism displayed in Figure 2 was found to be feasible. The process starts by forming **IM3** in which $B(C_6F_5)_3$ of **4** can avoid crashing with $B(C_6F_5)_3$ of **2**. Subsequently, **IM3** walks through **TS3** to reach **IM4**. From **IM3** to **TS3** to **IM4**, among the three bonds in the O···Si···H··· B linkage, the O−Si bond gradually shortens from 2.982 to 2.247 to 1.882 Å, the Si−H bond elongates from 1.620 to 1.779 to 2.422 Å, and the B−H bond shortens from 1.387 to 1.316 to 1.223 Å. These bond-length alternations describe a S_N2 process for formation of the complex **IM4**.

The system involves Lewis acid $B(C_6F_5)_3$, and **2** is a nucleophile with an exposed O atom. We examined the stability of the dative complex between **2** and $B(C_6F_5)_3$ because a very stable complex like this may disable catalysis. Piers et al. were able to obtain the X-ray structure of such a complex (i.e., **3X-ray** in Figure 2).[14] Again, the M05-2X optimized structure of the complex (**3**) is more compact than the X-ray structure (see Figure 2), implying overestimation of the nonbonding interaction by the functional, as mentioned above. The complex is 12.6 kcal/mol more stable than **2** + $B(C_6F_5)_3$; thus, **3** is stable enough for experimental capture. However, because the process **2** → **IM3** → **TS3** → **IM4** is kinetically very favorable with a

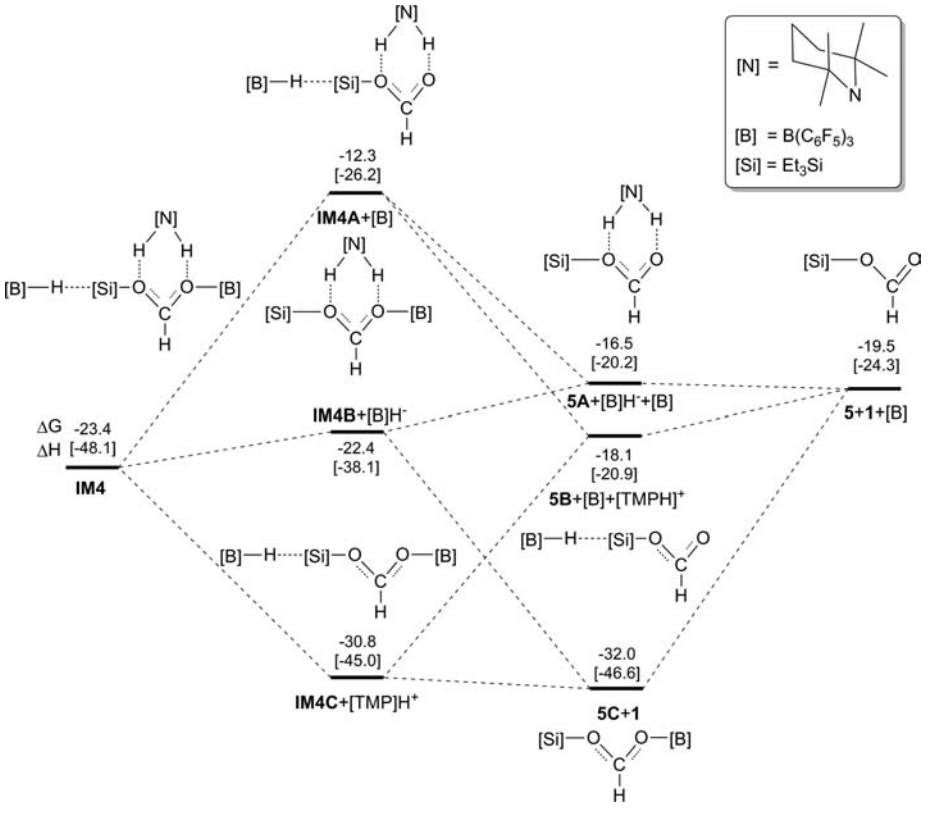

Figure 3. Thermodynamics (in kcal/mol) for the rearrangements of **IM4** to regenerate the catalyst **1**.

dx.doi.org/10.1021/ic401920b | *Inorg. Chem.* 2013, 52, 12098−12107

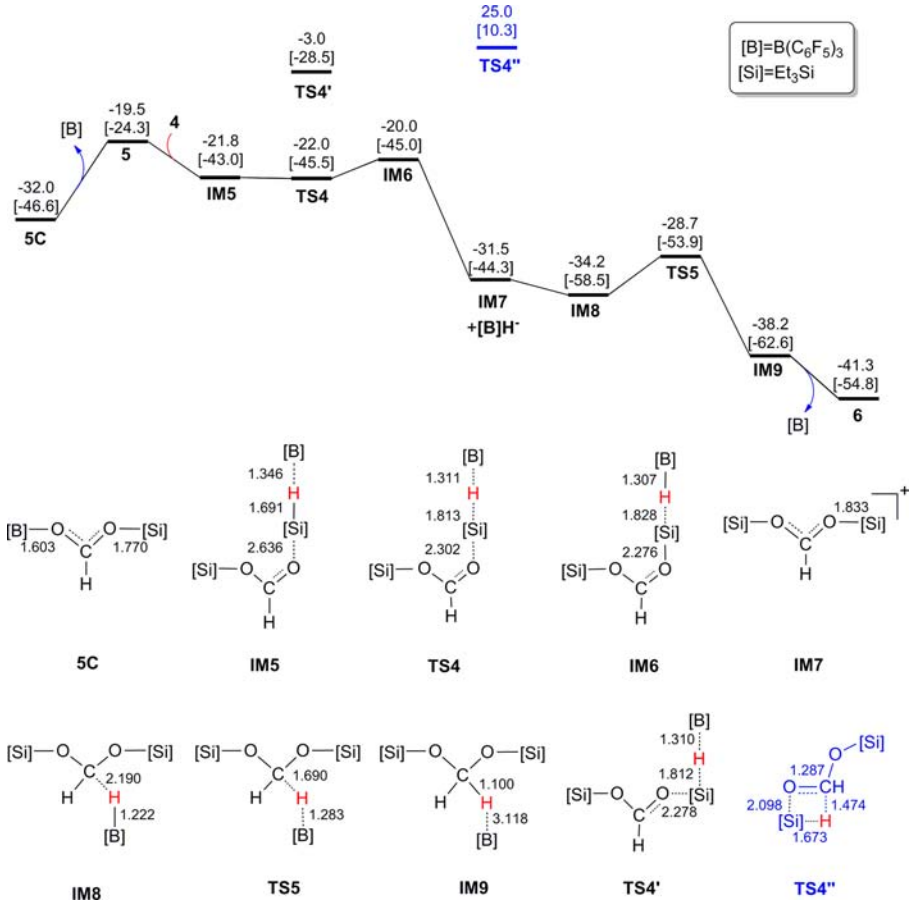

Figure 4. Free-energy (in kcal/mol) profile for the hydrosilylation of **5**, giving **6**, along with the optimized structures of the stationary points. Key bond lengths are given in angstroms.

barrier of less than 4.0 kcal/mol, even if including the energy cost for dissociation of **3** into **2** + $B(C_6F_5)_3$, the effective barrier for the process is only 16.5 kcal/mol (the energy difference between **3** and **TS3**), which is kinetically accessible. Therefore, **2** is available via microscopic equilibrium. Furthermore, as will be seen, the whole transformation from CO_2 + $4Et_3SiH$ to CH_4 + $2(Et_3SiO)_2O$ is highly exergonic by 132.7 kcal/mol, which provides a great thermodynamic force to drive the equilibrium toward dissociation of **3** into **2** + $B(C_6F_5)_3$.

The above S_N2 process results in **IM4**. As shown by its structure (see Figure 2), **IM4** is composed of four components (i.e., $B(C_6F_5)_3$, $[TMPH]^+$, **5**, and $[HB(C_6F_5)_3]^-$) binding together via nonbonding interactions. It is reasonable to assume that the four components can be rearranged facilely to form new structures. We did not attempt to locate the possible TSs for the rearrangements. Figure 3 examines the thermodynamics of the possible rearrangements via only breaking of the nonbonding interactions. In the three possible pathways that only dissociate one nonbonding component, the one resulting in $[TMPH]^+$ + **IM4C** is most favorable with the release of 7.4 kcal/mol free energy, while the dissociations of $[HB(C_6F_5)_3]^-$ and $B(C_6F_5)_3$ are uphill by 1.0 and 11.1 kcal/mol, respectively. Along the most favorable pathway, the resulting **IM4C** further dissociates into **5C** and $[HB(C_6F_5)]^-$. The latter can favorably (by 1.2 kcal/mol) bind to $[TMPH]^+$ to regenerate the catalyst **1**. The rearrangement from **IM4** to **5C** + **1** is overall exergonic by 8.6 kcal/mol; thus, the catalyst **1** can be recovered from **IM4** rearrangement energetically feasibly.

Stage III: Three Sequential $H^{\delta-}$ Transfer Steps. The complex **5C** obtained from **IM4** rearrangement has no exposed O atom available. In order to effectively react with **4**, we hypothesized that $B(C_6F_5)_3$ in **5C** can be dissociated, giving **5**. Indeed, the dissociation is feasible, costing only 12.5 kcal/mol, which is less than 12.6 kcal/mol for the dissociation of $B(C_6F_5)_3$ from **3** (see above). Figure 4 shows the pathway for the hydrosilylation of **5** mediated by $B(C_6F_5)_3$, which takes place via two sequential S_N2 processes. The first S_N2 process (**5** → **IM5** → **TS4** → **IM6**) proceeds via **5** attacking **4**, transferring $H^{\delta-}$ of Et_3SiH to $B(C_6F_5)_3$ to give **IM6** in which the Si−H and B−H distances are 1.828 and 1.307 Å, respectively. Note that **TS4** being lower than **IM5** and **IM6** is due to the solvent effect and thermal corrections. In terms of the gas-phase electronic energies, **TS4** is 2.4 and 0.1 kcal/mol higher than **IM5** and **IM6**, respectively. The favorable entropy drives the nonbonding complex (**IM6**) to separate, leading to more stable (11.5 kcal/mol) **IM7** and $[HB(C_6F_5)_3]^-$. The energetic results shown in the figure indicate that the S_N2 process is very feasible. After the first S_N2 process, the resulting $[HB(C_6F_5)_3]^-$ species roams to attack the electrophilic **IM7** at the C^{CO_2} center. By passing through **IM8**, **TS5**, and **IM9**, $H^{\delta-}$ of $[HB(C_6F_5)_3]^-$ transfers to the C^{CO_2} center, completing $H^{\delta-}$ transfer from Et_3SiH to CO_2, giving **6** and recovering the $B(C_6F_5)_3$ catalyst. Including the dissociation process of **5C** to **5** + $B(C_6F_5)_3$, the effective barrier (i.e., relative to **5C**) for the hydrosilylation of **5** is 12.5 kcal/mol and the process is exergonic by 9.3 kcal/mol. Note that no TS for **5C** dissociation could exist, as indicated by the potential energy surface scanned

dx.doi.org/10.1021/ic401920b | *Inorg. Chem.* 2013, 52, 12098−12107

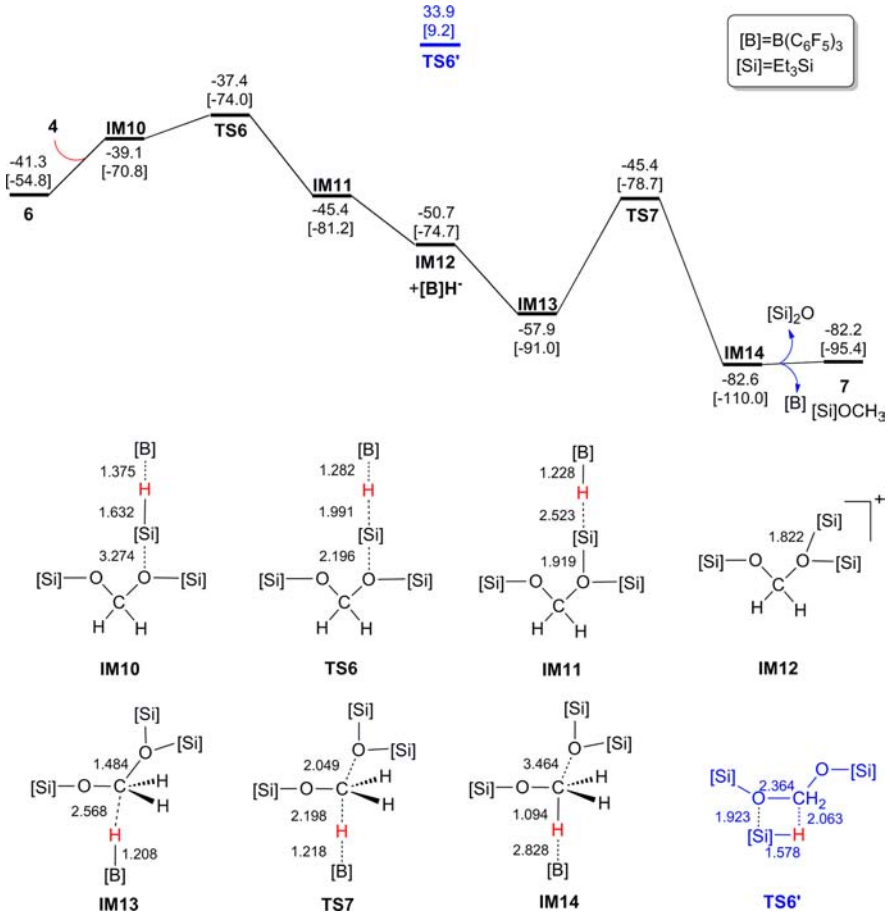

Figure 5. Free-energy (in kcal/mol) profile for the hydrosilylation of **6**, giving **7**, along with the optimized structures of the stationary points. Key bond lengths are given in angstroms.

by using the R−O bond distance as the reaction coordinate (see the Supporting Information).

In the above hydride-transfer mechanism, the first S_N2 process completely liberates $[HB(C_6F_5)_3]^-$, which needs to move around to find the electrophilic C^{CO_2} center. Alternatively, in this step, we were able to locate the TS for the least-motion pathway (i.e., the attacking model b mentioned above). In this least-motion pathway, as shown by **TS4′**, after the Si−O bond is formed, the leaving $[HB(C_6F_5)_3]^-$ can attack the electrophilic C^{CO_2} center with the least motion. **TS4′** is 19.0 kcal/mol higher than **TS4**, indicating that the pathway is less favorable than the one discussed above. Even in this unfavorable pathway, the catalytic effect of $B(C_6F_5)_3$ in facilitating the hydrosilylation is obvious. Without the assistance of $B(C_6F_5)_3$, the direct hydrosilylation of **5** via **TS4″** is very unfavorable, with **TS4″** being 28.0 kcal/mol higher than **TS4′**.

Continuing the reduction to the **6** level, two hydride-transfer steps occur, giving **7** and then CH_4. The two steps follow a mechanism similar to that from **5** to **6** (Figure 4), also involving two separate S_N2 processes. We show the energetic and geometric results of the two steps in Figures 5 and 6, respectively. The first hydride transfer has barriers of 3.9 and 12.5 kcal/mol for the two S_N2 processes, respectively, and the second one has barriers of 2.0 and 14.8 kcal/mol, respectively. The two hydride-transfer steps are exergonic by 40.9 and 50.5 kcal/mol, respectively. In the two steps, the direct hydride transfers via **TS6′** and **TS8′** are much less favorable than the $B(C_6F_5)_3$-mediated ones. We also examined the stability of the dative bonding complexes of $B(C_6F_5)_3$ with **6**, **7**, and $(Et_3Si)_2O$, respectively. The binding energies for the three complexes are even positive, being 7.5, 6.5, and 8.7 kcal/mol. Therefore, the species **6**, **7**, and $(Et_3Si)_2O$ can exist freely.

Putting the pathways in Figures 1, 2, and 4−6 together, it is clear that the rate-determining step for the whole transformation lies in the CO_2 activation with a barrier of 26.8 kcal/mol. The whole transformation is strongly exergonic by 132.7 kcal/mol. Therefore, the conversion can take place energetically feasibly. The various O−B dative complexes are not stable enough to prevent the conversion.

3.2. Comparisons to NHC- and [Ni]H-Catalyzed CO_2 Reductions. We previously investigated the mechanisms of [Ni]H- and NHC-catalyzed CO_2 reductions. Using HBcat and silanes (e.g., Ph_2SiH_2, denoted as [Si]H hereafter) as the reductants, respectively, the two catalytic systems convert CO_2 to $[Si]OCH_3$ and $catBOCH_3$, which can afford methanol after hydrolysis. In comparison, the present system also passes $[Si]OCH_3$ but completely reduces CO_2 into CH_4. It is interesting to compare the mechanistic differences among the three catalytic systems. For the [Ni]H and NHC systems, the conversion undergoes three hydride-transfer steps, sequentially transferring $H^{\delta-}$ from the hydrogen source (HBcat or silane) to CO_2 via the reducing sequence, $CO_2/CO_2 \rightarrow HC(=O)OBcat/H(C=O)O[Si] \rightarrow CH_2O/CH_2O \rightarrow catBOCH_3/[Si]OCH_3$. The catalysts [Ni]H and NHC participate in each of the three hydride-transfer steps with the same mechanism. Note that, for the two systems, the CO_2 activation mechanism

dx.doi.org/10.1021/ic401920b | Inorg. Chem. 2013, 52, 12098−12107

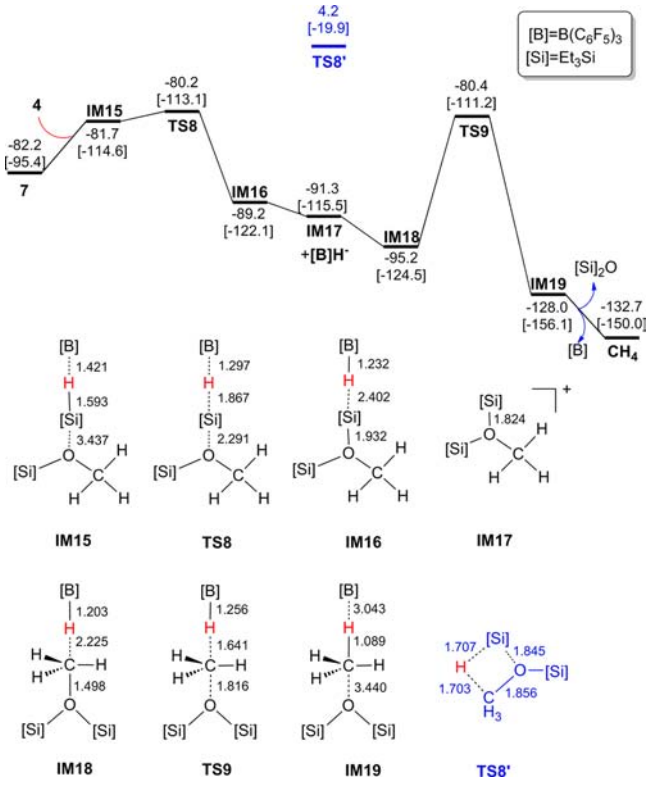

Figure 6. Free-energy (in kcal/mol) profile for the hydrosilylation of **7**, giving CH_4, along with the optimized structures of the stationary points. Key bond lengths are given in angstroms.

is the same as that for the subsequent two hydride-transfer steps. Using the first hydride-transfer step (i.e., CO_2 activation) as a representative, parts A and B of Scheme 2 describe the hydride-transfer mechanisms for the two systems, respectively. In the [Ni]H system, the hydride-transfer takes place via two processes, including the CO_2 insertion into the [Ni]H Ni−H bond, giving HCOO[Ni] and metathesis between HCOO[Ni] and HBcat, regenerating the [Ni]H catalyst and producing H(C═O)OBcat. In the NHC system, the catalyst NHC promotes the insertion of CO_2 into the Si−H bond via mode I or II. Note that the mode II was computationally shown to be less favorable than mode I, and we will not consider the mode II hereafter. Clearly, a requirement for such hydride-transfer mechanisms via insertion is that the hydride acceptor must feature a C═O double bond. Indeed, the hydride acceptors involved in the two reductions, including CO_2 and the partially reduced CO_2 intermediates (H(C═O)OBcat/H(C═O)O[Si] and CH_2O), meet the requirement. After the three hydride-transfer steps, the resultant $catBOCH_3$ and $[Si]OCH_3$ no longer possess C═O double bonds. We do not expect that the C−O single bonds in $catBOCH_3$ and $[Si]OCH_3$ can undergo similar insertions. Computationally, we were not able to locate an insertion TS similar to $\mathbf{TS1}^{[Ni]H}$–$\mathbf{TS3}^{[Ni]H}$ (Figure 7) for the insertion of $catBOCH_3$ into the [Ni]H Ni−H bond. Instead, we located $\mathbf{TS4}^{[Ni]H}$, which corresponds to a S_N2 TS and is 46.5 kcal/mol higher than $catBOCH_3$ + [Ni]H. In comparison, the corresponding values (corrected by using Martin et al.'s method[20]) for the insertions of CO_2, HC(═O)OBcat, and CH_2O into the [Ni]H Ni−H bond are 14.7, 28.2, and 18.7 kcal/mol, respectively. For the NHC system, we located $\mathbf{TS4}^{NHC}$ (Figure 7). Because $\mathbf{TS4}^{NHC}$ is structurally similar to $\mathbf{TS1}^{NHC}$–$\mathbf{TS3}^{NHC}$ for $H^{\delta-}$ transfer to CO_2, HC(═O)O[Si], and CH_2O, $\mathbf{TS4}^{NHC}$ is 50.5 kcal/mol higher than NHC + [Si]H + $[Si]OCH_3$, which is much larger than the corresponding values (22.0, 29.0, and 17.2 kcal/mol, corrected by using Martin et al.'s method[20]) for $\mathbf{TS1}^{NHC}$–$\mathbf{TS3}^{NHC}$, respectively. The much higher barriers of $\mathbf{TS4}^{[Ni]H}/\mathbf{TS4}^{NHC}$ than $\mathbf{TS1}^{[Ni]H}$–$\mathbf{TS3}^{[Ni]H}/\mathbf{TS1}^{NHC}$–$\mathbf{TS3}^{NHC}$ can be rationalized as follows. For the [Ni]H and NHC systems, because the hydride acceptors (CO_2, HC(═O)OBcat/HC(═O)O[Si], and CH_2O) possess C═O double bonds, the O atom of the C═O bond can easily bond to the Ni/Si center during insertion. In contrast, hydride transfer via $\mathbf{TS4}^{[Ni]H}/\mathbf{TS4}^{NHC}$ requires breaking of the C−O bonds of $catBOCH_3$ and $[Si]OCH_3$, which costs much more energy.

For the present system, the CO_2 activation and hydride-transfer steps follow different mechanisms. For the CO_2 activation, as sketched in Scheme 2C, $H^{\delta+}$ and $H^{\delta-}$ of **1** transfer to CO_2 to form a complex (i.e., **IM2**) with a well-formed HCOOH entity, followed by formation of the O−B dative bond, which drives HCOOH O−H bond breaks to return $H^{\delta+}$ to TMP. Exemplified by Scheme 2D, the subsequent hydride-transfer steps use $B(C_6F_5)_3$ as a hydride carrier to transfer hydride from the hydrogen source (i.e., Et_3SiH) to the C^{CO_2} center. $B(C_6F_5)_2$ first grabs a hydride from Et_3SiH with the assistance of **4** and then leaves it to the C^{CO_2} center via the S_N2 mechanism. Essentially, the S_N2 mechanism utilizes the nucleophilic O and electrophilic C centers in the hydride acceptors. It is not necessary for the hydride acceptors to have a C═O double bond. The species **6** and **7** do not have C═O double bonds but still feature electrophilic O and nucleophilic C to promote the S_N2 process, thus being able to complete hydride transfer until CO_2 is fully reduced to CH_4.

4. CONCLUSIONS

In summary, we have carried out M05-2X density functional theory computations to understand the detailed mechanism of the metal-free CO_2 reduction to CH_4 with Et_3SiH, catalyzed by an ammonium hydridoborate ion pair (**1**) in combination with $B(C_6F_5)_3$. The study confirms the mechanism proposed by Piers et al.[14] to be energetically feasible. The CO_2 reduction to CH_4 proceeds via CO_2 insertion into **1**, followed by three sequential hydride transfers from Et_3SiH to the C^{CO_2} center. In addition to rationalizing the experiment, the detailed mechanistic computations disclose information that cannot be observed experimentally. For the CO_2 activation by **1**, the insertion of CO_2 into the H−B bond of **1** takes place stepwise, with $H^{\delta+}$ and $H^{\delta-}$ of **1** first transferring to CO_2 to form a complex (**IM12**) with a HCOOH entity, and then the complex breaking the O−H bond, driven by formation of the O−B dative bond to return the cleaved $H^{\delta+}$ to TMP. The direct insertion of CO_2 into the H−B bond of **1** is highly unfavorable. The formed HCOOH entity cannot be liberated but offers a detour for the CO_2 insertion to the H−B bond of **1**. $B(C_6F_5)_3$ plays an important role in promoting hydride transfer, serving as a shuttle to bring $H^{\delta-}$ from Et_3SiH to CO_2. Each hydride transfer proceeds via two separate S_N2 processes. Aided by the nucleophilic attack of hydride acceptors, $B(C_6F_5)_3$ first grabs a hydride from Et_3SiH to form $[HB(C_6F_5)_3]^-$, which then leaves $H^{\delta-}$ to the electrophilic C^{CO_2} center. The mechanism is different from that used by [Ni]H- and NHC-mediated CO_2 reduction, which requires the hydride acceptors to have C═O double bonds. The differences explain why the present system can reduce CO_2 to CH_4, while the [Ni]H and NHC systems can only reduce CO_2 to $catBOCH_3$ and $[Si]OCH_3$.

dx.doi.org/10.1021/ic401920b | Inorg. Chem. 2013, 52, 12098−12107

Scheme 2. Comparisons of the Mechanisms for CO_2 Activation and Hydride Transfer in the [Ni]H (A), NHC (B), and Present Systems (C and D)

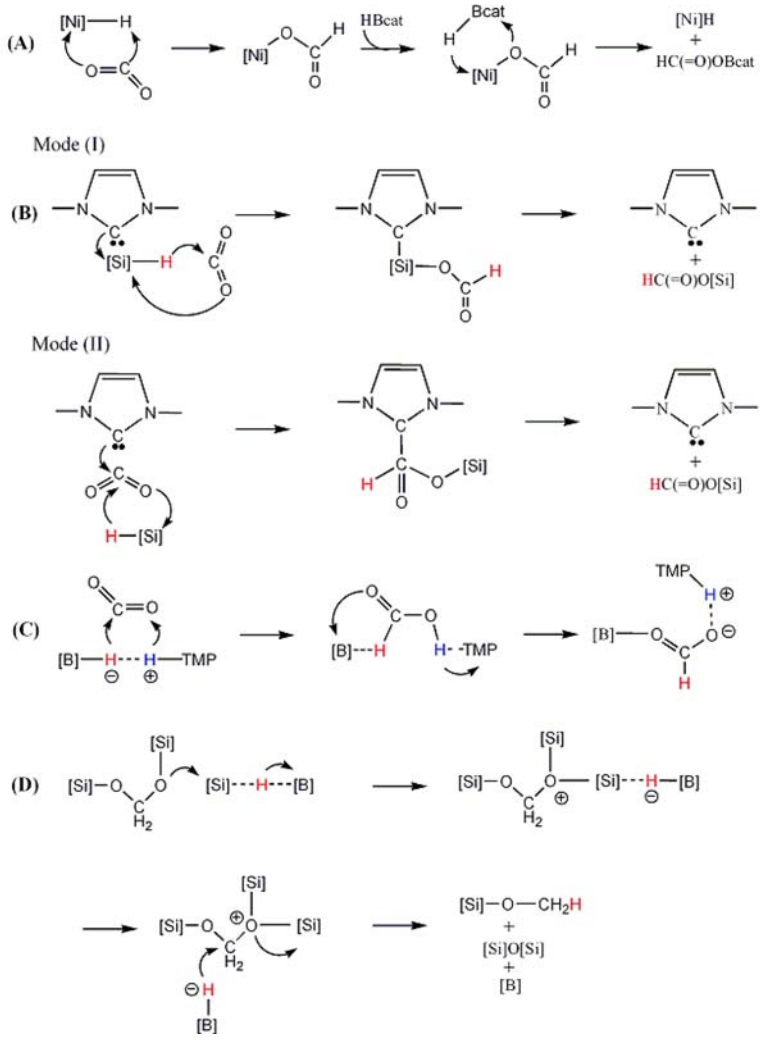

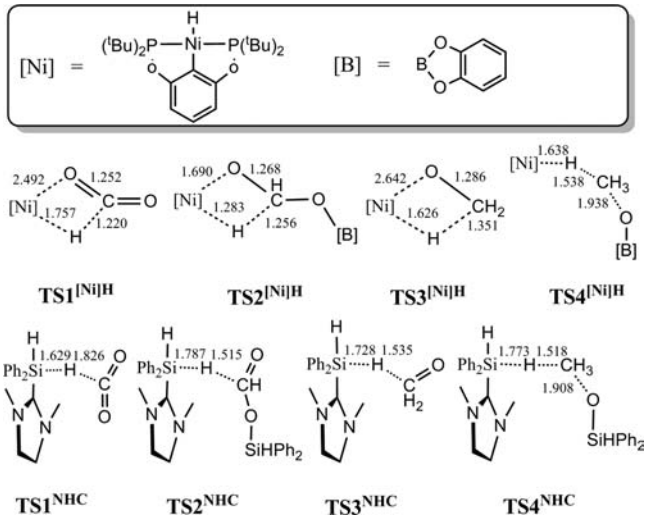

Figure 7. Optimized structures of the TSs involving [Ni]H/HBcat/CO_2 ($\mathbf{TS1}^{[Ni]H}$–$\mathbf{TS4}^{[Ni]H}$) and NHC/CO_2/[Si]H) ($\mathbf{TS1}^{NHC}$–$\mathbf{TS4}^{NHC}$) ([Si] = Ph_2SiH) systems. Key bond lengths are given in angstroms.

■ ASSOCIATED CONTENT

Supporting Information

Potential energy surface scanned using the B–O bond distance as the reaction coordinate and absolute enthalpies and Gibbs free energies and Cartesian coordinates of all of the structures involved in this study. This material is available free of charge via the Internet at http://pubs.acs.org.

■ AUTHOR INFORMATION

Corresponding Author

*E-mail: zxwang@ucas.ac.cn.

Notes

The authors declare no competing financial interest.

■ ACKNOWLEDGMENTS

This work is financially supported by National Natural Science Foundation of China (Grants 21173263 and 21373216).

■ REFERENCES

(1) For reviews on CO_2 transformations, see: (a) Wang, W.; Wang, S. P.; Ma, X. B.; Gong, J. L. *Chem. Soc. Rev.* **2011**, *40*, 3703–3727. (b) Quadrelli, E. A.; Centi, G.; Duplan, J. L.; Perathoner, S. *ChemSusChem* **2011**, *4*, 1194–1215. (c) Kember, M. R.; Buchard, A.; Williams, C. K. *Chem. Commun.* **2011**, *47*, 141–163. (d) Riduan, S.

N.; Zhang, Y. G. *Dalton Trans.* **2010**, *39*, 3347−3357. (e) Mikkelsen, M.; Jorgensen, M.; Krebs, F. C. *Energy Environ. Sci.* **2010**, *3*, 43−81. (f) Darensbourg, D. J. *Inorg. Chem.* **2010**, *49*, 10765−10780. (g) Sakakura, T.; Kohno, K. *Chem. Commun.* **2009**, 1312−1330. (h) Olah, G. A.; Goeppert, A.; Prakash, G. K. S. *J. Org. Chem.* **2009**, *74*, 487−498. (i) Yu, K. M. K.; Curcic, I.; Gabriel, J.; Tsang, S. C. E. *ChemSusChem* **2008**, *1*, 893−899. (j) Sakakura, T.; Choi, J. C.; Yasuda, H. *Chem. Rev.* **2007**, *107*, 2365−2387. (k) Darensbourg, D. J. *Chem. Rev.* **2007**, *107*, 2388−2410. (l) Aresta, M.; Dibenedetto, A. *Dalton Trans.* **2007**, 2975−2992. (m) Olah, G. A. *Angew. Chem., Int. Ed.* **2005**, *44*, 2636−2639. (n) Coates, G. W.; Moore, D. R. *Angew. Chem., Int. Ed.* **2004**, *43*, 6618−6639. (o) Arakawa, H.; Aresta, M.; Armor, J. N.; Barteau, M. A.; Beckman, E. J.; Bell, A. T.; Bercaw, J. E.; Creutz, C.; Dinjus, E.; Dixon, D. A.; Domen, K.; DuBois, D. L.; Eckert, J.; Fujita, E.; Gibson, D. H.; Goddard, W. A.; Goodman, D. W.; Keller, J.; Kubas, G. J.; Kung, H. H.; Lyons, J. E.; Manzer, L. E.; Marks, T. J.; Morokuma, K.; Nicholas, K. M.; Periana, R.; Que, L.; Rostrup-Nielson, J.; Sachtler, W. M. H.; Schmidt, L. D.; Sen, A.; Somorjai, G. A.; Stair, P. C.; Stults, B. R.; Tumas, W. *Chem. Rev.* **2001**, *101*, 953−996. (p) Drees, M.; Cokoja, M.; Kuhn, F. E. *ChemCatChem* **2012**, *4*, 1703−1712. (q) Fan, T.; Chen, X. H.; Lin, Z. Y. *Chem. Commun.* **2012**, *48*, 10808−10828. (r) Cheng, D. J.; Negreiros, F. R.; Apra, E.; Fortunelli, A. *ChemSusChem* **2013**, *6*, 944−965.

(2) For recent experimental studies of CO_2 conversion, see: (a) Buchard, A.; Kember, M. R.; Sandeman, K. G.; Williams, C. K. *Chem. Commun.* **2011**, *47*, 212−214. (b) Ren, W. M.; Zhang, X.; Liu, Y.; Li, J. F.; Wang, H.; Lu, X. B. *Macromolecules* **2010**, *43*, 1396−1402. (c) Rankin, M. A.; Cummins, C. C. *J. Am. Chem. Soc.* **2010**, *132*, 10021−10023. (d) Langer, J.; Imhof, W.; Fabra, M. J.; Garcia-Orduna, P.; Gorls, H.; Lahoz, F. J.; Oro, L. A.; Westerhausen, M. *Organometallics* **2010**, *29*, 1642−1651. (e) Kember, M. R.; White, A. J. P.; Williams, C. K. *Macromolecules* **2010**, *43*, 2291−2298. (f) He, C.; Tian, G.; Liu, Z. W.; Feng, S. H. *Org. Lett.* **2010**, *12*, 649−651. (g) Decortes, A.; Belmonte, M. M.; Benet-Buchholz, J.; Kleij, A. W. *Chem. Commun.* **2010**, *46*, 4580−4582. (h) Clegg, W.; Harrington, R. W.; North, M.; Pasquale, R. *Chem.—Eur. J.* **2010**, *16*, 6828−6843. (i) Sanz, S.; Benitez, M.; Peris, E. *Organometallics* **2010**, *29*, 275−277. (j) Federsel, C.; Boddien, A.; Jackstell, R.; Jennerjahn, R.; Dyson, P. J.; Scopelliti, R.; Laurenczy, G.; Beller, M. *Angew. Chem., Int. Ed.* **2010**, *49*, 9777−9780. (k) Zhuang, J.; Li, Z. H.; Fan, K. N. A.; Zhou, M. F. *J. Phys. Chem. A* **2012**, *116*, 3388−3395. (l) Thammayongsy, Z.; Seda, T.; Zakharov, L. N.; Kaminsky, W.; Gilbertson, J. D. *Inorg. Chem.* **2012**, *51*, 9168−9170. (m) Li, J. Y.; Hermann, M.; Frenking, G.; Jones, C. *Angew. Chem., Int. Ed.* **2012**, *51*, 8611−8614. (n) Yonke, B. L.; Reeds, J. P.; Zavalij, P. Y.; Sita, L. R. *Angew. Chem., Int. Ed.* **2011**, *50*, 12342−12346. (o) Williams, V. A.; Manke, D. R.; Wolczanski, P. T.; Cundari, T. R. *Inorg. Chim. Acta* **2011**, *369*, 203−214. (p) Menard, G.; Stephan, D. W. *Angew. Chem., Int. Ed.* **2011**, *50*, 8396−8399. (q) Krogman, J. P.; Foxman, B. M.; Thomas, C. M. *J. Am. Chem. Soc.* **2011**, *133*, 14582−14585. (r) Kleeberg, C.; Cheung, M. S.; Lin, Z. Y.; Marder, T. B. *J. Am. Chem. Soc.* **2011**, *133*, 19060−19063. (s) Gau, D.; Rodriguez, R.; Kato, T.; Saffon-Merceron, N.; de Cozar, A.; Cossio, F. P.; Baceiredo, A. *Angew. Chem., Int. Ed.* **2011**, *50*, 1092−1096. (t) Chiang, P. C.; Bode, J. W. *Org. Lett.* **2011**, *13*, 2422−2425. (u) Silvia, J. S.; Cummins, C. C. *J. Am. Chem. Soc.* **2010**, *132*, 2169−2170. (v) Nair, V.; Varghese, V.; Paul, R. R.; Jose, A.; Sinu, C. R.; Menon, R. S. *Org. Lett.* **2010**, *12*, 2653−2655. (w) Gu, L. Q.; Zhang, Y. G. *J. Am. Chem. Soc.* **2010**, *132*, 914−915. (x) Shintani, R.; Nozaki, K. *Organometallics* **2013**, *32*, 2459−2462.

(3) For recent computational studies of CO_2 conversion, see: (a) Dang, L.; Lin, Z. Y.; Marder, T. B. *Organometallics* **2010**, *29*, 917−927. (b) Li, J.; Jia, G. C.; Lin, Z. Y. *Organometallics* **2008**, *27*, 3892−3900. (c) Lim, C. H.; Holder, A. M.; Musgrave, C. B. *J. Am. Chem. Soc.* **2013**, *135*, 142−154. (d) Ahlquist, M. S. G. *J. Mol. Catal. A: Chem.* **2010**, *324*, 3−8. (e) Getty, A. D.; Tai, C. C.; Linehan, J. C.; Jessop, P. G.; Olmstead, M. M.; Rheingold, A. L. *Organometallics* **2009**, *28*, 5466−5477. (f) Li, J.; Lin, Z. Y. *Organometallics* **2009**, *28*, 4231−4234. (g) Brookes, N. J.; Ariafard, A.; Stranger, R.; Yates, B. F. *J. Am. Chem. Soc.* **2009**, *131*, 5800−5808. (h) Zhao, H. T.; Lin, Z. Y.; Marder, T. B. *J. Am. Chem. Soc.* **2006**, *128*, 15637−15643. (i) Ariafard, A.; Zarkoob, F.; Batebi, H.; Stranger, R.; Yates, B. F. *Organometallics* **2011**, *30*, 6218−6224. (j) Yang, X. *ACS Catal.* **2011**, *1*, 849−854. (j) Batebia, H.; Zarkooba, F.; Daraeia, K.; Yates, B. F.; Ariafard, A., *J. Organomet. Chem.* (**2013**), http://dx.doi.org/10.1016/j.jorganchem.2013.04.060. (k) Zimmerman, P. M.; Zhang, Z.; Musgrave, C. B. *Inorg. Chem.* **2010**, *49*, 8724−8728. (l) Lim, C.-H.; Holder, A. M.; Hynes, J. T.; Musgrave, C. B. *Inorg. Chem.* **2013**, *52*, 10062−10066.

(4) For representaive studies, see: (a) Schafer, A.; Saak, W.; Haase, D.; Muller, T. *Angew. Chem., Int. Ed.* **2012**, *51*, 2981−2984. (b) Han, Z. B.; Rong, L. C.; Wu, J.; Zhang, L.; Wang, Z.; Ding, K. L. *Angew. Chem., Int. Ed.* **2012**, *51*, 13041−13045. (c) Eisenschmid, T. C.; Eisenberg, R. *Organometallics* **1989**, *8*, 1822−1824. (d) Tominaga, K.; Sasaki, Y.; Kawai, M.; Watanabe, T.; Saito, M. *J. Chem. Soc., Chem. Commun.* **1993**, 629−631. (e) Wesselbaum, S.; vom Stein, T.; Klankermayer, J.; Leitner, W. *Angew. Chem., Int. Ed.* **2012**, *51*, 7499−7502. (f) Fachinetti, G.; Floriani, C.; Chiesivilla, A.; Guastini, C. *J. Am. Chem. Soc.* **1979**, *101*, 1767−1775. (g) Bontemps, S.; Vendier, L.; Sabo-Etienne, S. *Angew. Chem., Int. Ed.* **2012**, *51*, 1671−1674. (h) Menard, G.; Stephan, D. W. *J. Am. Chem. Soc.* **2010**, *132*, 1796−1797. (i) Chan, B.; Radom, L. *J. Am. Chem. Soc.* **2008**, *130*, 9790−9799. (j) Chan, B.; Radom, L. *J. Am. Chem. Soc.* **2006**, *128*, 5322−5323. (k) Roy, L.; Zimmerman, P. M.; Paul, A. *Chem.—Eur. J.* **2011**, *17*, 435−439. (l) Riduan, S. N.; Ying, J. Y.; Zhang, Y. G. *ChemCatChem* **2013**, *5*, 1490−1496. (l) Huff, C. A.; Sanford, M. S. *J. Am. Chem. Soc.* **2011**, *133*, 18122−18125. (m) Marc-André Courtemanche, M.-A.; Légaré, M.-A.; Maron, M.; Fontaine, F. G. *J. Am. Chem. Soc.* **2013**, *135*, 9326−9329.

(5) (a) Gambarotta, S.; Strologo, S.; Floriani, C.; Chiesivilla, A.; Guastini, C. *J. Am. Chem. Soc.* **1985**, *107*, 6278−6282. (b) Fachinetti, G.; Floriani, C.; Roselli, A.; Pucci, S. *J. Chem. Soc., Chem. Commun.* **1978**, 269−270.

(6) Chakraborty, S.; Zhang, J.; Krause, J. A.; Guan, H. R. *J. Am. Chem. Soc.* **2010**, *132*, 8872−8873.

(7) Riduan, S. N.; Zhang, Y. G.; Ying, J. Y. *Angew. Chem., Int. Ed.* **2009**, *48*, 3322−3325.

(8) Ashley, A. E.; Thompson, A. L.; O'Hare, D. *Angew. Chem., Int. Ed.* **2009**, *48*, 9839−9843.

(9) Huang, F.; Lu, G.; Zhao, L. L.; Li, H. X.; Wang, Z. X. *J. Am. Chem. Soc.* **2010**, *132*, 12388−12396.

(10) Huang, F.; Zhang, C. G.; Jiang, J. L.; Wang, Z. X.; Guan, H. R. *Inorg. Chem.* **2011**, *50*, 3816−3825.

(11) Matsuo, T.; Kawaguchi, H. *J. Am. Chem. Soc.* **2006**, *128*, 12362−12363.

(12) Park, S.; Bezier, D.; Brookhart, M. *J. Am. Chem. Soc.* **2012**, *134*, 11404−11407.

(13) Mitton, S. J.; Turculet, L. *Chem.—Eur. J.* **2012**, *18*, 15258−15262.

(14) Berkefeld, A.; Piers, W. E.; Parvez, M. *J. Am. Chem. Soc.* **2010**, *132*, 10660−10661.

(15) Khandelwal, M.; Wehmschulte, R. J. *Angew. Chem., Int. Ed.* **2012**, *51*, 7323−7326.

(16) (a) Stephan, D. W.; Erker, G. *Angew. Chem., Int. Ed.* **2010**, *49*, 46−76. (b) Stephan, D. W. *Org. Biomol. Chem.* **2008**, *6*, 1535−1539. (c) Stephan, D. W. *Dalton Trans.* **2009**, 3129−3136. (d) Kenward, A. L.; Piers, W. E. *Angew. Chem., Int. Ed.* **2008**, *47*, 38−41. (e) *Topics in Current Chemistry: Frustrated Lewis Pair I*; Erker, G.; Stephan, D. W., Eds.; Springer: Berlin, 2013; Vol. *332* (the complete issue).

(17) (a) Wang, Z.-X.; Zhao, L.; Lu, G.; Li, H.; Huang, F. *Top. Curr. Chem.* **2013**, *332*, 231−266. (b) Wang, Z. X.; Lu, G.; Li, H. X.; Zhao, L. L. *Chin. Sci. Bull.* **2010**, *55*, 239−245. (c) Lu, G.; Li, H. X.; Zhao, L. L.; Huang, F.; Wang, Z. X. *Inorg. Chem.* **2010**, *49*, 295−301. (d) Zhao, L. L.; Li, H. X.; Lu, G.; Wang, Z. X. *Dalton Trans.* **2010**, *39*, 4038−4047. (e) Li, H. X.; Zhao, L. L.; Lu, G.; Huang, F.; Wang, Z. X. *Dalton Trans.* **2010**, *39*, 5519−5526. (f) Zhao, L. L.; Lu, G.; Huang, F.; Wang, Z. X. *Dalton Trans.* **2012**, *41*, 4674−4684. (g) Lu, G.; Li, H. X.; Zhao, L. L.; Huang, F.; Schleyer, P. V.; Wang, Z. X. *Chem.—Eur. J.* **2011**, *17*, 2038−2043.

(18) Zhao, Y.; Truhlar, D. G. *J. Chem. Phys.* **2006**, 125.

(19) Marenich, A. V.; Cramer, C. J.; Truhlar, D. G. *J. Phys. Chem. B* **2009**, *113*, 6378−6396.
(20) Martin, R. L.; Hay, P. J.; Pratt, L. R. *J. Phys. Chem. A* **1998**, *102*, 3565−3573.
(21) (a) Huang, D.; Makhlynets, O. V.; Tan, L. L.; Lee, S. C.; Rybak-Akimova, E. V.; Holm, R. H. *Inorg. Chem.* **2011**, *50*, 10070−10081. (b) Huang, D. G.; Makhlynets, O. V.; Tan, L. L.; Lee, S. C.; Rybak-Akimova, E. V.; Holm, R. H. *Proc. Natl. Acad. Sci. U. S. A.* **2011**, *108*, 1222−1227.
(22) (a) Carpenter, J. E.; Weinhold, F. *THEOCHEM* **1988**, *46*, 41−62. (b) Reed, A. E.; Weinhold, F. *J. Chem. Phys.* **1983**, *78*, 4066−4073. (c) Foster, J. P.; Weinhold, F. *J. Am. Chem. Soc.* **1980**, *102*, 7211−7218.
(23) Frisch, M. J.; Trucks, G. W.; Schlegel, H. B.; Scuseria, G. E.; Robb, M. A.; Cheeseman, J. R.; Scalmani, G.; Barone, V.; Mennucci, B.; Petersson, G. A.; Nakatsuji, H.; Caricato, M.; Li, X.; Hratchian, H. P.; Izmaylov, A. F.; Bloino, J.; Zheng, G.; Sonnenberg, J. L.; Hada, M.; Ehara, M.; Toyota, K.; Fukuda, R.; Hasegawa, J.; Ishida, M.; Nakajima, T.; Honda, Y.; Kitao, O.; Nakai, H.; Vreven, T.; Montgomery, J. A., Jr.; Peralta, J. E.; Ogliaro, F.; Bearpark, M.; Heyd, J. J.; Brothers, E.; Kudin, K. N.; Staroverov, V. N.; Kobayashi, R.; Normand, J.; Raghavachari, K.; Rendell, A.; Burant, J. C.; Iyengar, S. S.; Tomasi, J.; Cossi, M.; Rega, N.; Millam, J. M.; Klene, M.; Knox, J. E.; Cross, J. B.; Bakken, V.; Adamo, C.; Jaramillo, J.; Gomperts, R.; Stratmann, R. E.; Yazyev, O.; Austin, A. J.; Cammi, R.; Pomelli, C.; Ochterski, J. W.; Martin, R. L.; Morokuma, K.; Zakrzewski, V. G.; Voth, G. A.; Salvador, P.; Dannenberg, J. J.; Dapprich, S.; Daniels, A. D.; Farkas, Ö.; Foresman, J. B.; Ortiz, J. V.; Cioslowski, J.; Fox, D. J. *Gaussian 09*; Gaussian, Inc.: Wallingford, CT, 2009.
(24) Tran, S. D.; Tronic, T. A.; Kaminsky, W.; Heinekey, D. M.; Mayer, J. M. *Inorg. Chim. Acta* **2011**, *369*, 126−132.
(25) (a) Chakraborty, S.; Patel, Y. J.; Krause, J. A.; Guan, H. R. *Polyhedron* **2012**, *32*, 30−34. (b) Federsel, C.; Jackstell, R.; Beller, M. *Angew. Chem., Int. Ed.* **2010**, *49*, 6254−6257. (c) Schlorer, N. E.; Cabrita, E. J.; Berger, S. *Angew. Chem., Int. Ed.* **2002**, *41*, 107−109. (d) Schlorer, N. E.; Berger, S. *Organometallics* **2001**, *20*, 1703−1704. (e) Schmeier, T. J.; Hazari, N.; Incarvito, C. D.; Raskatov, J. A. *Chem. Commun.* **2011**, *47*, 1824−1826. (f) Johnson, M. T.; Johansson, R.; Kondrashov, M. V.; Steyl, G.; Ahlquist, M. S. G.; Roodt, A.; Wendt, O. F. *Organometallics* **2010**, *29*, 3521−3529. (g) Wu, J. G.; Green, J. C.; Hazari, N.; Hruszkewycz, D. P.; Incarvito, C. D.; Schmeier, T. J. *Organometallics* **2010**, *29*, 6369−6376.
(26) (a) Parks, D. J.; Blackwell, J. M.; Piers, W. E. *J. Org. Chem.* **2000**, *65*, 3090−3098. (b) Parks, D. J.; Piers, W. E. *J. Am. Chem. Soc.* **1996**, *118*, 9440−9441. (c) Chojnowski, J.; Rubinsztajn, S.; Cella, J. A.; Fortuniak, W.; Cypryk, M.; Kurjata, J.; Kazmierski, K. *Organometallics* **2005**, *24*, 6077−6084.
(27) (a) Thompson, D. B.; Brook, M. A. *J. Am. Chem. Soc.* **2008**, *130*, 32−33. (b) Sumerin, V.; Schulz, F.; Nieger, M.; Leskela, M.; Repo, T.; Rieger, B. *Angew. Chem., Int. Ed.* **2008**, *47*, 6001−6003. (c) Blackwell, J. M.; Morrison, D. J.; Piers, W. E. *Tetrahedron* **2002**, *58*, 8247−8254.

■ NOTE ADDED AFTER ASAP PUBLICATION

This paper was published on the Web on October 2, 2013. Two additional citations were added to reference 3, and the corrected version was reposted on October 7, 2013.